Rab4 affects both recycling and degradative endosomal trafficking

Mary W. McCaffrey[a,*], Anna Bielli[a], Giuseppina Cantalupo[b], Silvia Mora[a], Vera Roberti[b], Mariarosaria Santillo[c], Frances Drummond[a], Cecilia Bucci[b,d]

[a] *Cell and Molecular Biology Laboratory, Biochemistry Department, UCC, Cork, Ireland*
[b] *Dipartimento di Biologia e Patologia Cellulare e Molecolare 'L. Califano' and C.E.O.S. 'G. Salvatore' del C.N.R., Università di Napoli 'Federico II', Via S. Pansini 5, 80131 Naples, Italy*
[c] *Dipartimento di Neuroscienze e della Comunicazione Interumana, Università di Napoli 'Federico II', Via S. Pansini 5, 80131 Naples, Italy*
[d] *Dipartimento di Biologia, Università di Lecce, Via Monteroni, 73100 Lecce, Italy*

Received 19 December 2000; revised 1 March 2001; accepted 15 March 2001

First published online 3 April 2001

Edited by Felix Wieland

Abstract The small GTPases Rab4, Rab5 and Rab7 are endosomal proteins which play important roles in the regulation of various stages of endosomal trafficking. Rab4 and Rab5 have both been localized to early endosomes and have been shown to control recycling and endosomal fusion, respectively. Rab7, a marker of the late endosomal compartment, is involved in the regulation of the late endocytic pathway. Here, we compare the role of Rab4, Rab5 and Rab7 in early and late endosomal trafficking in HeLa cells monitoring ligand uptake, recycling and degradation. Expression of the Rab4 dominant negative mutant (Rab4AS22N) leads to a significant reduction in both recycling and degradation while, as expected, Rab7 mutants exclusively affect epidermal growth factor (EGF) and low density lipoprotein degradation. As also expected, expression of the dominant negative Rab5 mutant perturbs internalization kinetics and affects both recycling and degradation. Expression of Rab4WT and dominant positive mutant (Rab4AQ67L) changes dramatically the morphology of the transferrin compartment leading to the formation of membrane tubules. These transferrin positive tubules display swellings (varicosities) some of which are positive for early endosomal antigen-1 and contain EGF. We propose that the Rab4GTPase is important for the function of the early sorting endosomal compartment, affecting trafficking along both recycling and degradative pathways.

Key words: Endocytosis; Low density lipoprotein; Epidermal growth factor; Transferrin; Rab GTPase; Membrane trafficking

1. Introduction

Eukaryotic receptor-mediated endocytosis is a fundamental cellular process whereby ligands, bound with a high degree of specificity to cell surface receptors, are internalized as part of the plasma membrane lipid bilayer [1]. This event is accomplished by the formation of clathrin coated pits leading to the generation of clathrin coated vesicles which 'pinch off' into the cell. The internalized clathrin coated vesicle is then uncoated and the receptor/ligand complexes are transported to early endosomes (EE) [2] which function as the primary sorting location in this pathway [3,4]. In the early/sorting endosome, molecules destined for degradation are sorted towards the late endosome and molecules destined for recycling are transported either directly back to the plasma membrane (fast recycling) or indirectly via the perinuclear 'recycling compartment' (RC) [5–7]. Despite the fact that the molecular events underlying such transport steps are unclear, the kinetics of endocytic trafficking of several markers such as transferrin (Tfn), epidermal growth factor (EGF) and low density lipoprotein (LDL) have been well documented and a number of proteins are known to be involved in these transport events [8,9]. One group of proteins which are necessary for efficient membrane transport through both the biosynthetic and endocytic route are the Rab GTPases, for reviews see [10–14]. The Rab proteins form the most extensive branch of the ras GTPase superfamily [15], are localized to distinct organelles of the biosynthetic and endocytic pathways, and are implicated in the control of membrane trafficking at specific steps. For example, Rab4, Rab5, and Rab11 are localized to EE and serve different functions. Rab4 has been shown to be involved in the regulation of recycling from the EE and, in particular, Tfn receptor (TfR) recycling [16,17]. Rab5 is important in the homotypic fusion between EE as well as in the transport to the early endosomal compartment [18–20]. In addition, it seems to be also necessary for budding of vesicles from the plasma membrane and has been suggested to regulate transport beyond EE [21]. Rab11, on the other hand, has been demonstrated to function in transport through the RC [22,23]. Two Rab proteins are localized to the late endosomal compartment, Rab7 and Rab9 [24,25]. Rab7 has been shown to control late endocytic trafficking [26–29] while Rab9 regulates transport from late endosomes to the *trans* Golgi network [25]. In the early endosomal pathway, Rab4 and Rab5 appear to function sequentially, since increased expression of Rab5 leads to an increase in fluid phase and receptor-mediated endocytosis and generates enlarged EE, suggesting that Rab5 regulates the clathrin coated pathway of receptor internalization and transport into the EE [19,20]. On the other hand, cells overexpressing Rab4 exhibit normal kinetics of endocytosis but display a reduced steady state of fluid phase markers and an accumulation of TfR on the cell surface [17]. Rab4 has therefore been implicated in the regulation of membrane recycling from the EE to the RC or directly to the plasma membrane [30]. Rab4 has not been found on late endosomes or co-localizing with Rab7 [31] also arguing for Rab4 function at a location prior to the late endosomal compartment.

*Corresponding author. Fax: (353)-21-4274034.
E-mail: m.mccaffrey@ucc.ie

PII: S0014-5793(01)02359-6

In order to better understand Rab4 function, we monitored the effects of expression of different Rab4 mutants on Tfn, LDL and EGF uptake and recycling. Furthermore, we examined Rab4 effects on LDL and EGF degradation. We then compared the Rab4 data with Rab5 and Rab7 function in the endocytic pathway. Tfn, EGF and LDL are commonly used physiological endocytic markers which bind to their respective receptors on the cell surface. Subsequent to binding, the ligand–receptor complex is internalized via clathrin coated pits. In the early sorting endosome the EGF and LDL dissociate from their respective receptors and the bulk of these ligands is then delivered to the late/degradative compartments. Tfn, on the other hand, is the classical recycling marker which is transported (with its receptor) to the cell surface, either directly or via the perinuclear RC. The data presented here demonstrate that the (GDP-locked) dominant negative Rab4S22N mutant leads to a substantial reduction in both recycling and degradation.

In addition to the quantitative assays, we qualitatively monitored the effect of the expression of the Rab4 mutants on the distribution of the TfR positive compartment by immunofluorescence techniques. In these experiments, we observed morphological abnormalities of the early (Tfn positive) endosomal compartment upon expression of Rab4. The most dramatic of which are detected on expression of Rab4WT and the dominant positive (GTPase deficient) Rab4Q67L mutant, where we visualize the formation of a Tfn positive membrane tubular structure. On the other hand, Rab4S22N leads to the formation of a more vesicular perinuclear Tfn positive compartment.

Since expression of Rab4GDP reduces recycling and degradation of endocytic markers, we propose a role for the Rab4GTPase in the organization/function of the early sorting endosome.

2. Materials and methods

2.1. Plasmids

The *myc*-tagged Rab5 and Rab7WT and mutant plasmids used in these studies have been previously described [20,28]. PGEM*myc*-Rab4AWT and pGEM*myc*-Rab4AQ67L, were obtained by subcloning the respective Rab4 cDNAs as *Eco*RI–*Sal*I fragments from pLexARab4AWT and pLexARab4A Q67L [32] into the *Eco*RI–*Sal*I-digested pGEM*myc*. pGEM*myc*-Rab4AS22N was constructed by two stage PCR amplification of Rab4A, using Rab4A in pUC8 [33] as a template with the primer Rab4A-ATG+*Bam*HI (5′-ACTAGTGCGGATCCTCCGAAACCTACGATTTTTTGT-3′) and the primer Rab4AS22N (5′-GAAGTAAGCAATTTTTGCCAGTTCC-3′) creating the mutation. This first round PCR product was then used as a primer together with a pUC8 specific downstream primer (5′-GTGCCAAGCTTGGCTGC-3′) and the full length Rab4AS22N PCR product was cloned into the *Bam*HI site of pBTM116 (pLex). The Rab4AS22N cDNA fragment was subcloned from this source into pGEM*myc* as an *Eco*RI–*Sal*I fragment.

2.2. Cell culture and transient transfection

Tissue culture reagents were from Gibco BRL and Biowhittaker. HeLa cells were grown in DMEM supplemented with 10% FCS, 2 mM glutamine, 100 U/ml penicillin and streptomycin and grown in a 5% CO_2 incubator at 37°C. HeLa cells were infected with either the MVA T7 vaccinia virus [34] or the vT7 recombinant vaccinia virus and transfected as described [19,35]. The transfection reagent was either DOSPER or DOTAP obtained from Boehringer Mannheim. Cells were transfected for 9–10 h and then processed for immunofluorescence, fluorescent marker uptake or biochemical assays (gel electrophoresis and blotting or trafficking assays). For LDL or EGF quantitative trafficking assays, cells were transfected for 4–5 h before starting to internalize the endocytic markers. Samples were examined, in parallel, by immunofluorescence for expression of the transfected construct. Only samples with a transfection efficiency of 70%, or greater, were utilized in quantitative assays.

2.3. Antibodies

Rabbit polyclonal anti-Rab4 serum was prepared by immunizing rabbits (Biological Services Unit, UCC) with purified recombinant Rab4A protein and affinity-purified antibody was prepared. The resulting antibody, at a dilution of 1/200 detects as little as 10 ng Rab4p by Western blotting and did not detect any other Rab protein (Rab1, Rab3, Rab5 or Rab6) tested under the same conditions. Crude rabbit polyclonal anti-sera to the early endosomal antigen-1 (EEA1) was a kind gift of H. Stenmark and was utilized at a dilution of 1/1000 to detect the endogenous protein. A commercial mouse monoclonal anti-human TfR antibody (B3/25, Boehringer Mannheim) was utilized to detect the endogenous TfR by immunofluorescence.

2.4. Confocal immunofluorescence microscopy

Cells on 11 mm round glass coverslips were fixed with 3% paraformaldehyde and free aldehyde groups were quenched with 50 mM NH_4Cl. The fixed cells were then permeabilized, with 0.05% saponin or 0.1% Triton X-100 for 5 min and incubated with a rabbit anti-Rab4 or anti-EEA1 polyclonal antibodies and with a mouse anti-TfR monoclonal antibody, as primary antibodies. Secondary antibodies were Texas red (TxR) coupled donkey anti-rabbit and fluorescein isothiocyanate-coupled (FITC)-conjugated donkey anti-mouse IgG (Jackson Immunoresearch). Coverslips were mounted in Mowiol and examined on a Bio-Rad MRC 1024 Zeiss Axioskop confocal microscope with a 63×/1.40 plan-Apochromat lens. Samples were excited at wavelengths of 488 and 568 nm and images were processed using Adobe Photoshop 5.0 software.

2.5. Internalization of fluorescent markers

9 h post-transfection, serum-starved cells grown on glass coverslips, were incubated for 1 h at 37°C in the presence of 33 μg/ml FITC-Tfn and 3 μg/ml TxR-coupled EGF (TxR-EGF) from Molecular Probes. After fluorescent marker uptake, cells were washed briefly in cold PBS, fixed, quenched and mounted in Mowiol for microscopic examination, as above.

2.6. GTP overlay blot and immunoblot

HeLa cells were infected and transfected with pGEM*myc*Rab4 constructs, as above, and lysed 6 h later in 150 mM NaCl, 50 mM Tris (pH 8.0), 1% Triton X-100, 0.2% SDS, 0.5% sodium deoxycholate. Extracts (15 μg of total cellular protein) were resolved by electrophoresis on 12% SDS–polyacrylamide gels and transferred to nitrocellulose filters. After transfer, the blot was incubated in binding buffer (50 mM sodium phosphate pH 7.5, 10 μM $MgCl_2$, 2 mM DTT, 0.2% Tween 20, 4 μM ATP) for 30 min at room temperature (RT) followed by incubation for 1 h at RT in binding buffer containing ^{32}P-labelled GTP at 1 μCi/ml. Blots were then washed in binding buffer four times for 15 min by agitation and exposed to X-ray film. GTP overlay blots were stripped of bound GTP by washing the blot in exchange buffer (20 mM Tris–HCl pH 7.5, 1 mM EDTA, 1 mM DTT, 250 mM ammonium sulfate) followed by incubation for 1 h in (20 mM Tris–HCl pH 7.5, 5 mM $MgCl_2$, 1 mM EDTA, 50 mM NaCl, 1 mM DTT, 200 μM GDP). Nucleotide stripping was confirmed by autoradiography and the blot was developed with Rab4 antibodies by blocking and incubation with the primary antibody (rabbit anti-rab4 serum) at a 1/200 dilution. Filters were washed, incubated with a secondary anti-rabbit HRP-conjugated antibody for 1 h at RT and the bands were visualized using the enhanced chemiluminescence system (Pierce).

2.7. Estimation of ^{125}I-LDL internalization, recycling and degradation

Human LDL ($1.019 < d < 1.063$ g/ml) were obtained by preparative ultracentrifugation and labelled with ^{125}I as described [28]. The specific activity of ^{125}I-LDL ranged between 200 and 400 cpm/ng of protein: more than 98% ^{125}I radioactivity was precipitable by trichloroacetic acid (TCA) and less than 3% was extractable in chloroform–methanol. Radioiodinated LDL was always used within 2 weeks of preparation. Cells were incubated for 24 h in medium complemented with human lipoprotein deficient serum (LPDS) before transfection. Cells were then transfected with either the empty vector (control) or one of the Rab constructs and allowed to internalize ^{125}I-LDL

that was added to the medium at a concentration of 20 μg/ml for 5 h and the amount of ^{125}I-LDL surface bound, internalized and degraded was estimated as previously described [28]. To determine the amount of LDL recycled, cells were incubated for 30 min at 37°C in the presence of ^{125}I-LDL at a concentration of 20 μg/ml. Then the cells were washed extensively with PBS/0.1% bovine serum albumin (BSA) on ice and reincubated for 1 h in medium at 37°C. The medium was then collected and the TCA precipitable material (^{125}I-LDL recycled) was counted with a γ-counter. To measure kinetics of internalization, cells were incubated at 4°C in the presence of ^{125}I-LDL for 2 h, washed extensively with PBS/0.1% BSA on ice and then incubated in medium at 37°C for various times. The cells were then immediately transferred on ice, washed with cold PBS/0.1% BSA and then the amount of ^{125}I-LDL internalized was determined as described above.

2.8. Estimation of ^{125}I-EGF recycling and degradation

Human ^{125}I-EGF was purchased from Amersham Biotech. Cells transfected with either the empty vector (control) or one of the Rab constructs were incubated with 20 μg/ml of ^{125}I-EGF in medium lacking serum at 37°C for 30 min, washed extensively on ice with cold PBS/0.1% BSA and reincubated in medium without serum at 37°C for 1 h. The amount of ^{125}I-EGF degraded and recycled was determined as described [36]. To measure kinetics of internalization, cells were incubated for different time points (ranging from 1 to 10 min) in the presence of 40 μg/ml ^{125}I-EGF at 37°C. Cells were then chilled on ice, washed with cold PBS/0.1% BSA several times, once with PBS and treated with 3 mg/ml of pronase in serum-free medium containing 10 mM HEPES, pH 7.3 for 1 h at 0°C. The cells were recovered by centrifugation at 3000 rpm for 3 min. The radioactivity present in pellet (cell-associated) was detected with a γ-counter. Statistical differences were calculated using a Student *t*-test for unpaired data.

2.9. Other assays

Protein concentration was determined by a colorimetric method [37] with the reagent obtained from either Bio-Rad or BCA (Pierce); recrystallized BSA or immunoglobulin G (IgG) were used as standards.

3. Results

3.1. Expression of Rab proteins in transfected HeLa cells

We have used previously generated Rab5 and Rab7 mutated constructs encoding mutant proteins behaving as dominant negative (Rab5S34N, Rab7T22N) or constitutively active (Rab5Q79L, Rab7Q67L) [20,28]. Expression of these constructs in HeLa cells using the vaccinia T7 system resulted in a strong overexpression (>15 fold compared to endogenous level, data not shown). We describe here the generation and characterization of the equivalent Rab4A mutants, dominant negative (S22N) and constitutively activated (Q67L). In order to verify the biochemical behavior of the mutants, lysates from HeLa cells expressing the Rab4A constructs were analyzed by SDS–PAGE followed by GTP overlay and immunoblotting (Fig. 1). Cells were infected with vaccinia strain MVA T7 polymerase and transfected 30 min to 1 h later with pGEM*myc*Rab4WT or pGEM*myc*Rab4S22N or pGEM*myc*Rab4Q67L. After transfection, cells were incubated for a further 6 h to allow expression of the exogenous Rab4 construct. Untreated non-infected, non-transfected (NINT) HeLa cells were included as a negative control. 15 μg cell lysate from each sample was analyzed in the GTP overlay assay and, as expected, the Rab4S22N mutant was deficient in GTP binding, while wild type and constitutively activated Rab4 efficiently bound GTP (Fig. 1A). In order to confirm equivalent sample loading and expression of all Rab4 constructs, the GTP blot was stripped of nucleotide, stripping was verified by autoradiography, and developed as an immunoblot with a polyclonal anti-Rab4 serum (Fig. 1B). All Rab4 constructs are expressed at similar levels and vastly in excess of the endogenous protein (Fig. 1B). Under the conditions of the experiment endogenous Rab4 is not detectable by immunoblot, while a strong signal is obtained for all Rab4 constructs.

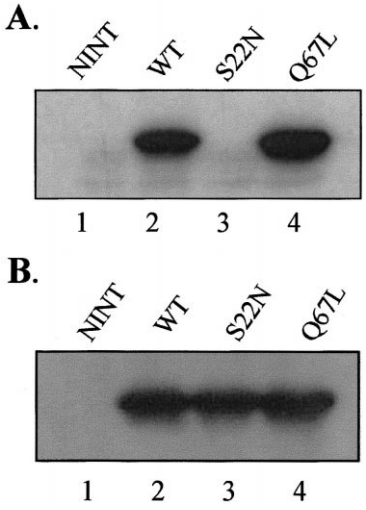

Fig. 1. GTP overlay assay (A) and immunoblot analysis (B) of HeLa cells transfected with Rab4WT and mutants. HeLa cells were infected with MVA T7, transfected with pGEM*myc*Rab4 constructs and lysed 6 h later. Samples (15 μg of protein) from untreated NINT HeLa cells (lane 1); or transfected Rab4WT (lane 2), Rab4S22N (lane 3), and Rab4Q67L (lane 4), were resolved on a 12% SDS–PAGE and transferred to nitrocellulose filters. The blot was incubated for 1 h in binding buffer containing ^{32}P-labelled GTP and exposed to X-ray film (A). The GTP blot was then stripped of nucleotide and developed using a rabbit anti-Rab4 polyclonal serum. Bands were visualized after incubation with anti-rabbit HRP-labelled secondary antibody and ECL (B).

3.2. Effects of Rab4, Rab5 and Rab7 mutant proteins on LDL kinetics of endocytosis

To compare the effect of overexpression of the different Rab4, Rab5 and Rab7WT and mutant proteins on LDL kinetics of uptake, we transfected HeLa cells for 4 h with the different constructs. We then incubated the cells at 4°C for 2hrs to allow binding of ^{125}I-LDL and then, after washing, reincubated the cells for different times at 37°C. As shown in Fig. 2 no effects on the internalization kinetics of ^{125}I-LDL were detected upon expression of Rab4 and Rab7 WT and mutant proteins (Fig. 2A,C). In contrast, Rab5WT and Rab5Q79L expression increased the amount of ^{125}I-LDL internalized (Fig. 2B), in agreement with previously published results that Rab5 expression alters the kinetics of endocytosis of ^{125}I-Tfn [19,20]. Conversely, expression of the Rab5 dominant negative mutant Rab5S34N inhibited the kinetics of endocytosis (Fig. 2B), again in agreement with previous studies [19,20]. However, while the kinetics of ^{125}I-Tfn endocytosis previously reported were dramatically altered by the expression of Rab5WT and mutant proteins in BHK21 cells [19,20], the kinetics of endocytosis of ^{125}I-LDL were altered to a lesser extent by Rab5WT and mutant proteins in this study utilizing HeLa cells (Fig. 2B) – probably a consequence of cell system experimental differences. Such differences have been previously reported in EGF internalization kinetics on Rab5 expression [36].

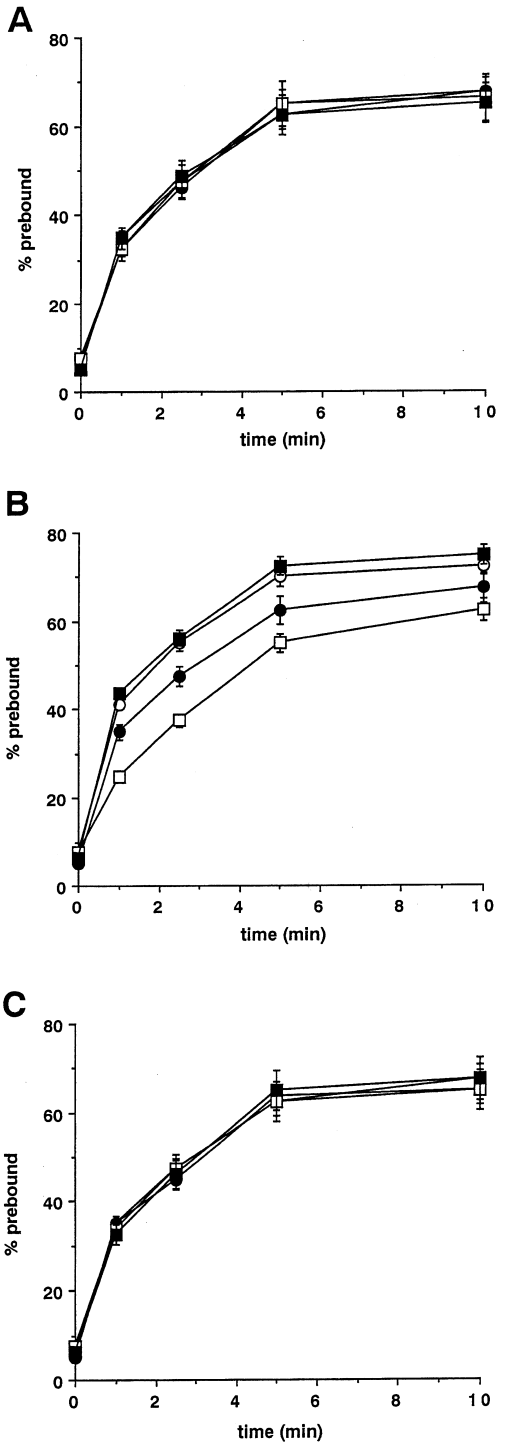

Fig. 2. Kinetics of ^{125}I-LDL uptake in cells expressing Rab4, Rab5 or Rab7. Cells were infected with the vT7 recombinant vaccinia virus and transfected with the different constructs as follows: A = Rab4; B = Rab5; C = Rab7. For each panel the following key applies: shaded circle = control cells (cells transfected with empty vector); unshaded circle = WT Rab; shaded box = dominant positive Rab mutant (Rab4Q67L, Rab5Q79L or Rab7Q67L); unshaded box = dominant negative Rab mutant (Rab4S22N, Rab5S34N or Rab7T22N). After 4 h of transfection, cells were washed extensively and incubated for 2 h at 4°C in the presence of 20 μg/ml of ^{125}I-LDL. Cells were then washed extensively at 4°C and reincubated at 37°C for various times. The amount of ^{125}I-LDL internalized is plotted as percentage of that prebound. The data with error bars represent the average of two independent (quadruple sample) experiments.

3.3. Effects of Rab4, Rab5 and Rab7 mutant proteins on recycling and degradation

We measured the amount of ^{125}I-Tfn, ^{125}I-LDL and ^{125}I-EGF recycled in cells expressing the different Rab constructs. 5 h after transfection, with empty vector or various Rab constructs, cells were allowed to internalize ^{125}I-LDL or ^{125}I-EGF for 30 min at 37°C, washed on ice extensively with cold PBS/0.1% BSA and then reincubated for 1 h at 37°C. The amount of ligand recycled in the medium was then quantified. ^{125}I-Tfn recycling was measured as previously described [17,19]. A strong inhibition in ligand recycling 30, 60 and 35% for Tfn, LDL and EGF respectively was evident when the dominant negative Rab4 mutant was expressed (data not shown). Consistent with this, overexpression of Rab4WT and of the constitutively active mutant Rab4Q67L caused an increase in the amount of recycled ligands. This increase however was small (max. 10%). As expected, the recycling of Tfn, LDL or EGF was not altered by the expression of Rab7WT or mutant proteins. In the case of Rab5, we observed an increase in recycling when the dominant negative mutant Rab5S34N was expressed, again in agreement with previously published data [36].

We also measured the amount of ^{125}I-LDL or ^{125}I-EGF degraded in HeLa cells transfected with the different Rab WT and mutant proteins. Cells which had been transiently transfected, with empty vector or various Rab constructs, for 4–5 h were incubated in the presence of ^{125}I-LDL or ^{125}I-EGF and the amount of both markers degraded was quantified as described in Section 2. The results of these experiments are shown in Fig. 3A,B. As expected, when the Rab7 dominant negative mutant was expressed degradation was severely impaired (75 and 65% for LDL and EGF, respectively). Degradation was also reduced (50%) in cells expressing Rab5S34N dominant negative mutant (Fig. 3) as a consequence of the inhibited internalization and of a diminished steady state pool of normally functioning EE due to increased recycling with this mutant (see Section 3.2). Surprisingly, however, when we looked at the effect of Rab4WT and mutant proteins on degradation we observed that expression of the dominant negative mutant strongly impaired degradation, 50 and 30% for LDL and EGF respectively (Fig. 3). In contrast, expression of Rab4WT or Rab4Q67L did not alter significantly degradation of either marker but caused a small (5–10%) but consistent increase in degradation.

3.4. Rab4WT and mutant expression affects the morphology of the TfR compartment

As Rab4 affected recycling and degradation of all ligands we tested whether expression of Rab4WT, Rab4Q67L and Rab4S22N caused changes in the morphology of the early endosomal compartment. We therefore monitored the distribution of the TfR as an early endosomal marker in HeLa cells transfected with the Rab4WT and mutant proteins (Fig. 4.I). Rab4 constructs were transiently overexpressed for 9 h by using the T7 RNA polymerase recombinant vaccinia virus system. The cells were prepared for immunofluorescence, and then double-stained with primary and secondary antibodies. Overexpressed Rab4 protein was detected by using an affinity-purified rabbit anti-Rab4 polyclonal antibody and visualized using a TxR-labelled anti-rabbit antibody (red), while the TfRs were detected with a mouse anti-human TfR monoclonal antibody and visualized with a FITC-labelled

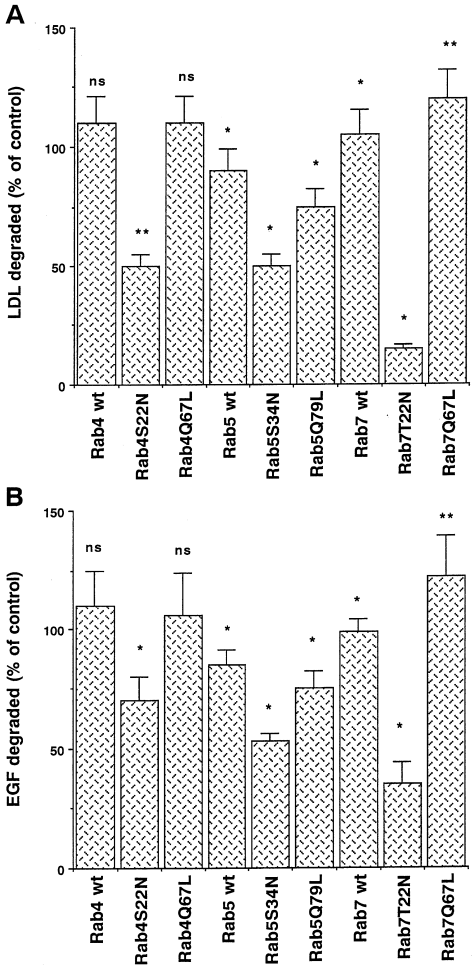

Fig. 3. Effect of Rab4, Rab5 and Rab7, WT and mutant proteins, on ^{125}I-LDL and ^{125}I-EGF degradation. Cells were infected with the vT7 recombinant vaccinia virus and transfected with the different constructs, or empty vector control, as indicated. After 4–5 h of transfection, cells were washed extensively and incubated for 30 min at 37°C in the presence of 20 μg/ml of ^{125}I-EGF or 5 h in the presence of 20 μg/ml of ^{125}I-LDL. The amount of ^{125}I-LDL (A) and of ^{125}I-EGF (B) degraded was estimated as described in Section 2 and plotted as percentage of control cells. The data represent the average of four independent experiments with error bars $*P < 0.001$; $**P < 0.005$; ns, not statistically significant, compared to control.

anti-mouse antibody (green). In mock-transfected cells (A,B) the TfR positive compartment showed typical vesicular structures dispersed throughout the cytoplasm and clusters of TfR containing vesicles more concentrated in the perinuclear area (B). In cells overexpressing Rab4WT or mutants (C,E,G) a diffuse red signal throughout the cell was visualized, indicating expression of exogenous Rab4. When Rab4WT (C,D) and Rab4Q67L (E,F) were overexpressed the distribution of TfR-labelled element was drastically altered, TfR-labelled elements were found in a tubular network. In contrast, cells overexpressing Rab4S22N (G,H) showed a vesicular staining for Tfn which was mainly concentrated in the perinuclear area. Some vesicles were also present peripherally in the cytoplasm but to a lesser extent than in mock-transfected cells. These results suggest that both the wild type and the active form of the Rab4 protein (Rab4Q67L) expand the morphology of the Tfn positive endosomes into a tubular membrane structure. Conversely, overexpression of the inactive form of Rab4 (Rab4S22N) appears to induce the accumulation of vesicles into a perinuclear area.

To further investigate the consequences of Rab4 expression on the early endosomal compartment we transfected HeLa cells, with the empty vector (Fig. 4.IIA–C), Rab4WT (D–F) or the Rab4S22N mutant (G–I) and monitored the EEA1 compartment morphology in parallel with TfR. Mock-transfected cells display a typical TfR compartment which co-localizes substantially with EEA1, as previously described [38]. Cells transfected with Rab4WT display a tubulated TfR compartment (D), with EEA1 localizing to this structure at distinct, often swollen, domains (varicosities) but not along the entire structure (E). On the other hand, in cells expressing Rab4S22N, EEA1 displayed a very fine vesicular pattern concentrating in a spherical fashion around the nucleus (H) and co-localizing substantially with TfR positive vesicles (G).

In order to further characterize the morphology and identity of the abnormal early endosomal compartment, generated on Rab4 overexpression, we monitored the localization of FITC-Tfn in parallel with TxR-EGF in mock-transfected cells (Fig. 4.IIIA–C) and cells expressing Rab4WT (D–F) or Rab4S22N (G–I). In control cells, a typical vesicular Tfn pattern was observed (A) while EGF labelled a less peripheral population of vesicles (B) and displayed partial co-localization with Tfn vesicles (C). EGF also partially co-localized with FITC-Tfn when either wild type or the dominant negative Rab4S22N mutant were expressed. However, the structures labelled differed. On Rab4WT expression EGF localized predominantly, but not exclusively, to varicosities of the abnormal Tfn compartment (E). On the other hand, when Rab4S22N is expressed, the EGF compartment displays a 'finer' punctate pattern (H) and a higher degree of co-localization with Tfn (compare I and C). To investigate the morphological effects more fully we have done pilot stereological analysis, using a simple point counting method, on the TxR-EGF signal in control vs. Rab4GDP expressing sample. The proportion (of cell volume) containing TxR-EGF in the Rab4GDP expressing sample is 2.6× greater than that of the (mock-transfected) control. We have also estimated the degree of co-localization of FITC-Tfn and Tx-EGF in the the mock-transfected control as compared with the S22N expressing sample. The control sample displays 10% co-localization while Rab4S22N displays 50% co-localization, consistent with the view that marker segregation is less efficient when Rab4GDP is expressed.

4. Discussion

Due to the complexity and dynamic nature of the endocytic compartment and its trafficking routes, we decided to study the effects of three small GTPases and mutants thereof in a single cell type by quantitative methods. In order to cover as comprehensively as possible all effects of these proteins on endocytosis and distinguish between direct and secondary effects, we followed quantitatively intake into the early endosomal compartment and exit from this compartment to both recycling and degradative routes, as well as monitoring the morphology of the endosomal compartment using early endosomal markers. Previous work from different laboratories has demonstrated that while Rab5 regulates the initial steps of transport to EE, Rab4 regulates recycling from this compartment and Rab7 the late steps of endocytosis [17,19,21,27,28].

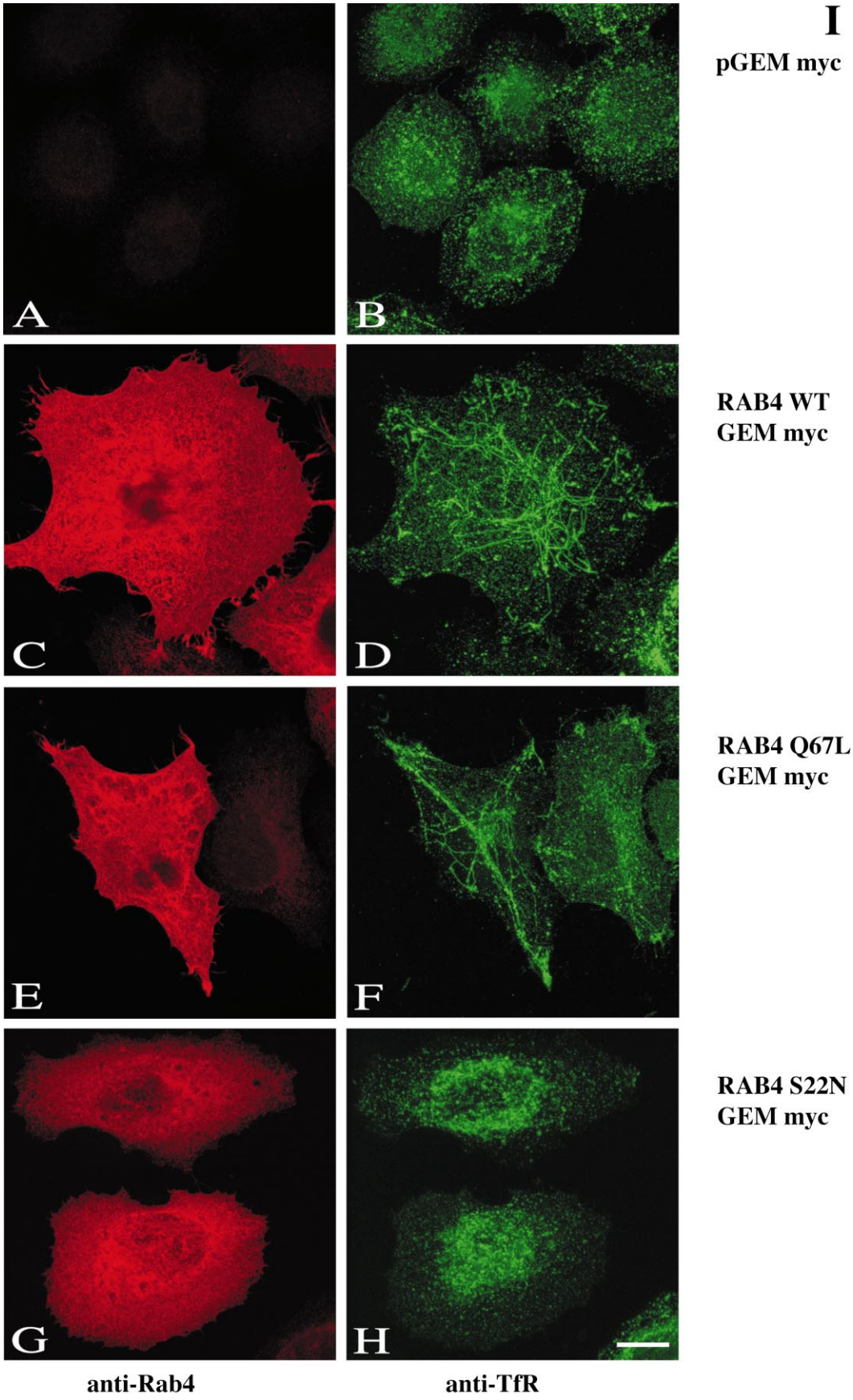
I
pGEM myc
A
B
RAB4 WT
GEM myc
C
D
RAB4 Q67L
GEM myc
E
F
RAB4 S22N
GEM myc
G
H
anti-Rab4
anti-TfR

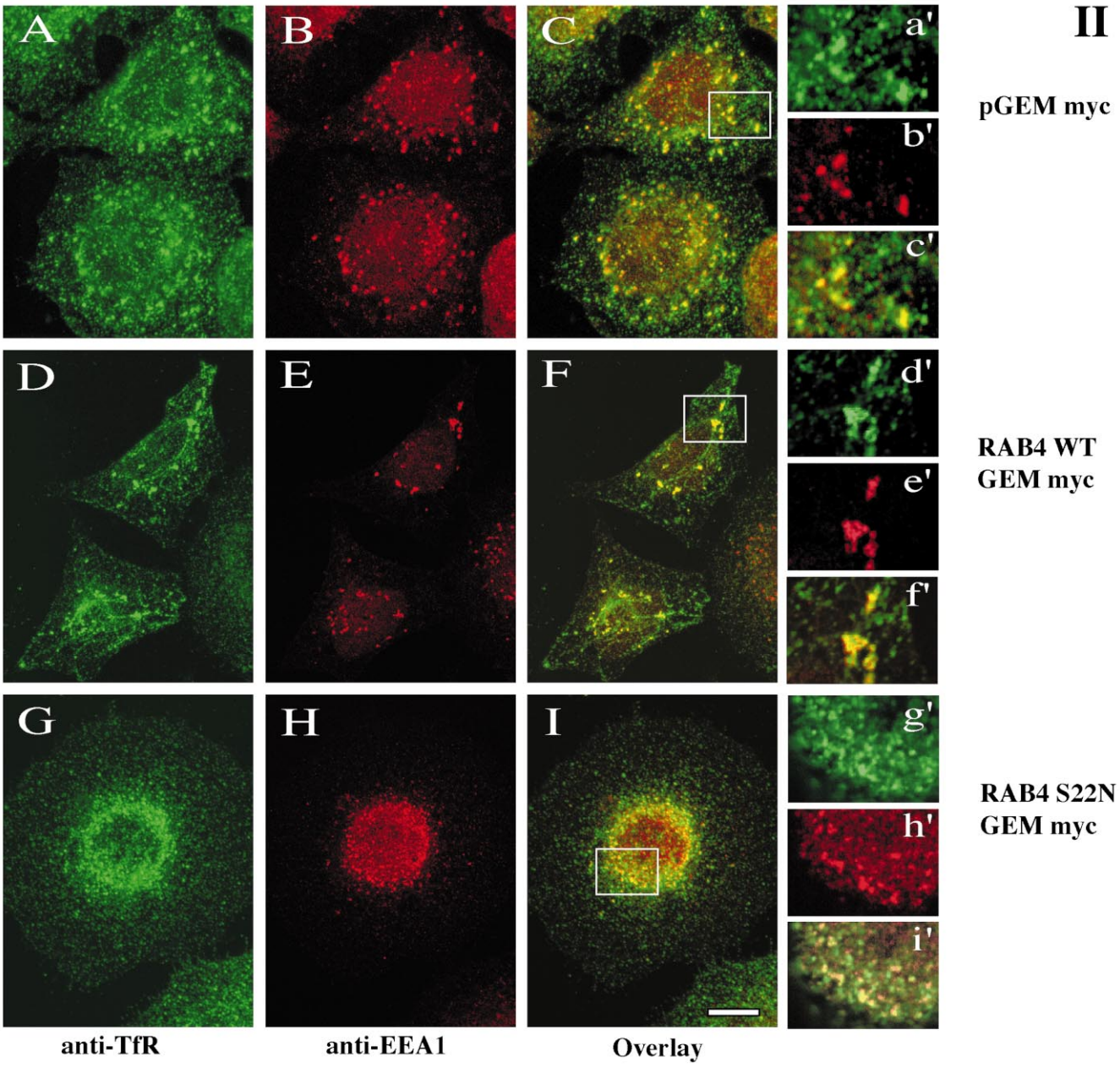

Fig. 4. Morphological alterations of the TfR compartment in HeLa cells overexpressing Rab4WT and mutants. I: HeLa cells were infected with MVA T7 and transfected for 9 h with empty vector pGEM*myc* (A,B), or with plasmids encoding Rab4WT (C,D), Rab4Q67L (E,F), or Rab4S22N (G,H). The cells were fixed, permeabilized and double-stained for confocal microscopy analysis with an affinity-purified rabbit anti-Rab4 polyclonal antibody, and with a mouse anti-TfR B3/25 monoclonal antibody. Cells were then visualized using TxR-labelled anti-rabbit IgG (red), and FITC-labelled anti-mouse IgG (green), as secondary antibodies. II: HeLa cells were infected and transfected with pGEM*myc* (A–C) or with plasmids encoding Rab4WT (D–F) or Rab4S22N (G–I) as above, and double-stained for confocal microscopy with mouse anti-TfR B3/25 monoclonal antibody and rabbit anti-EEA1 polyclonal antibody, as primary antibodies. Cells were then visualized using TxR-labelled anti-rabbit IgG (red), and FITC-labelled anti-mouse IgG (green), as secondary antibodies. A–I: Whole stack projections of the combined serial sections. White boxes identify selected areas for which a single section is shown (enlarged) on right, a′–i′. III (see next page): HeLa cells were infected and transfected with pGEM*myc* (A–C), Rab4WT (D–F) or Rab4S22N (G–I) as above, and then incubated with FITC-Tfn and TxR-EGF for 1 h at 37°C. A–I: Whole stack projections of the combined serial sections. White boxes identify selected areas for which a single section is shown (enlarged) on right, a′–i′. Scale bar represents 10 μm.

However, these studies were done in different cell lines utilizing different expression systems, different point mutants and analyzing different markers for endocytosis so it is difficult to directly compare the effect of the three proteins. Therefore, we considered it important to examine the function of these three Rab proteins in the same system, utilizing equivalent point mutations for all three Rabs and following three endocytic markers. In the quantitative assays, we examined the effect of Rab4, Rab5 and Rab7 wild type and mutant proteins on EGF and LDL degradation in HeLa cells. Furthermore, we examined Tfn, EGF and LDL recycling. We demonstrate that Rab4 affects degradative trafficking in addition to recycling. As expected, Rab7 only affected degradation, confirming that it controls late endocytic steps and the expression of the wild

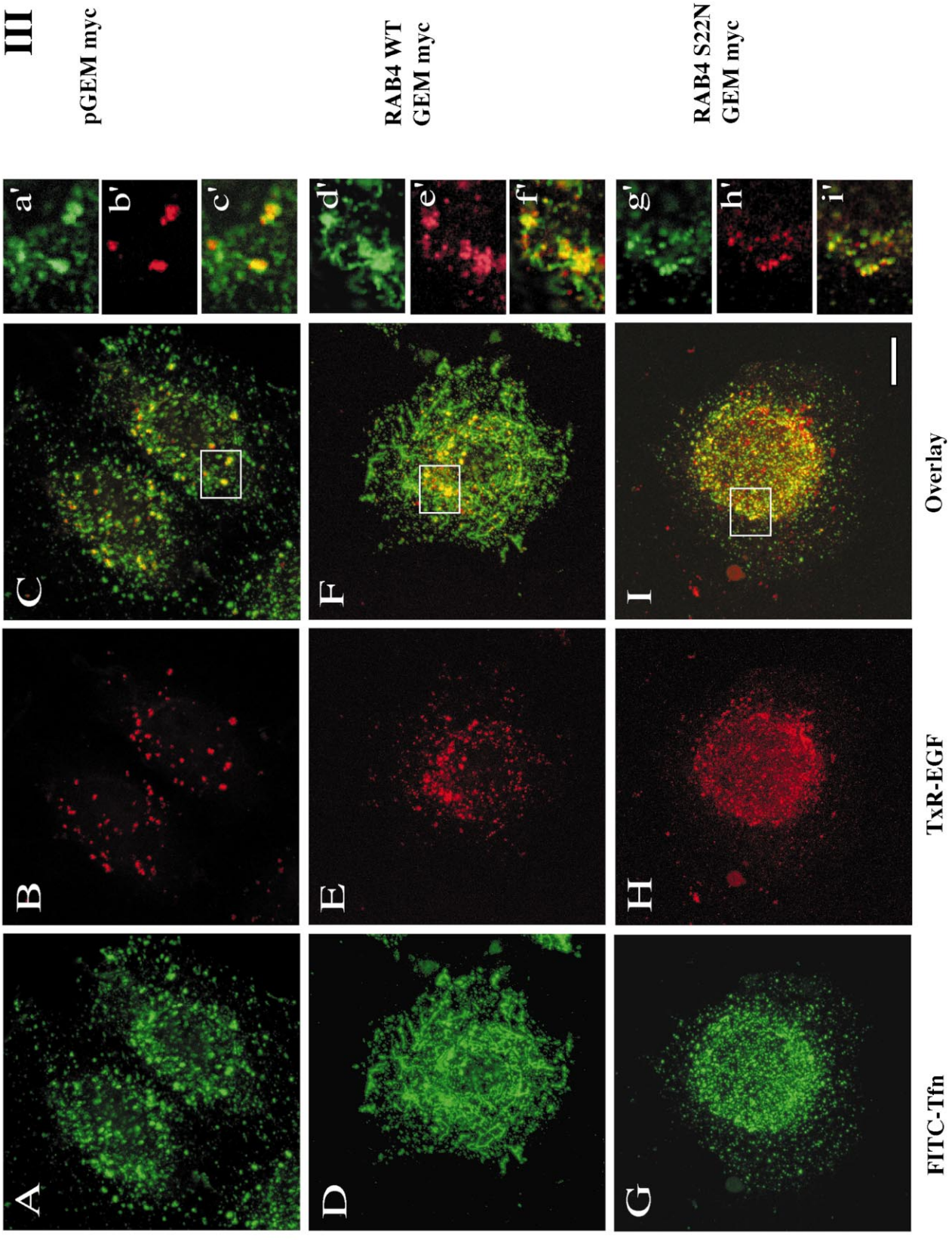

Fig. 4 (*continued*).

type or mutant proteins does not affect internalization or recycling rates, while Rab5 displays major effects on early endocytic events.

The Rab4 protein has been found to be associated with an early endosomal compartment clearly distinct from the late endosomal compartment, labelled by the Rab7 protein [16,30,31]. Moreover, Rab4 has been found to play an important role in the control of the Tfn recycling pathway [17]. We

show here that expression of the Rab4S22N dominant negative mutant (locked in the GDP-bound form) affects strongly not only recycling (reduced by 30–60%) but also degradation (reduced by 30–50%). Since the kinetics of internalization were not affected by expression of any of the Rab4 constructs, these data indicate that the Rab4 effect is not a consequence of altered uptake. Only a small increase (up to 10%) was observed in recycling and degradation in cells overexpressing Rab4 wild type and the active Rab4Q67L mutant. This minor effect of Rab4WT on the degradative endosomal pathway is consistent with a previous report on Rab4 function [17]. The substantial effects of the dominant negative Rab4S22N mutant, in this study, altering recycling and degradation suggest that Rab4 is important for sorting from the early endosomal compartment to both recycling and degradative routes.

The effects of Rab5 are consistent with that previously published, where it has been implicated in inward budding from the plasma membrane, in the fusion of endocytic vesicles with EE and in the homotypic fusion of EE [18,19,21].

Rab7 function, as expected, appears to be confined to the late steps of endocytosis since we observe no effects on the kinetics of uptake or recycling. Therefore, the Rab7 data presented here are consistent with previously published data implicating Rab7 in the late endosomal/degradative pathway [26,27,29].

We have also observed by immunofluorescence that the overexpression of the Rab4 protein results in morphological alterations to the TfR compartment. Expression of Rab4 mutants cause opposite morphological changes to this compartment. In cells overexpressing either the wild type or the active form of Rab4 (Rab4Q67L), the fTfR-labelled elements were distributed as a tubular network. In contrast, cells overexpressing the inactive form of Rab4 protein (Rab4S22N) showed vesicular staining for the TfR which was mainly concentrated in the perinuclear area. Despite the fact that the Rab4S22N effects on the TfR compartment are not so dramatic, we consistently observed this phenotype. Rab4 is believed to control recycling of TfR from the sorting endosomes back to the membrane, which can occur directly (fast cycle) or indirectly via the RC (slow cycle). The immunofluorescence results, suggest that both Rab4WT and Rab4Q67L proteins expand the morphology of the Tfn positive endosomes into a tubular membrane structure. Since Tfn is present in sorting endosomes, RC and recycling vesicles it is not possible to distinguish whether this structure is an abnormal sorting endosome, RC or a recycling vesicle. However, based on the localization of Rab4 already described [16,30,31,39,40] it is probable that this compartment is of either sorting endosome or RC nature. Considering published data on Rab4 localization [16,30,31,39,40] and function [17,41] and the effect of the Rab4S22N mutant on endosomal trafficking to the degradative pathway (described here), it is likely that the Rab4 effects are exerted on the sorting endosome rather than the RC. To better characterize this compartment, we investigated whether it is decorated by the early endosomal marker EEA1 and if it contains EGF. We show here that the Tfn positive structure, generated by Rab4 expression, is positive for both EEA1 and EGF with both markers decorating a subpopulation of the Tfn positive swellings/varicosities distributed along the membrane tubules caused by Rab4WT overexpression. The EEA1 signal appears to be perturbed on Rab4WT overexpression with fewer EEA1 structures labelled than in control cells, which display a multiple small vesicle pattern. The morphological effects generated by overexpression of wild type and Rab4Q67L proteins are likely to be due to an increased production of TfR-labelled membrane buds from the sorting endosome resulting in the observed formation of membrane tubules, as Rab4 augments the budding process from this compartment. Our quantitative results also support this theory, since a small (max. 10%) increase in recycling and degradation was observed on overexpression of wild type and Rab4Q67L proteins. The Rab4S22N protein is in a GDP-inactive state and, in our model would be expected to reduce exit from the sorting endosomes. The morphological and the quantitative data support this theory as we observe both an accumulation of vesicles containing TfR/FITC-Tfn, EEA1 and EGF in the perinuclear area, and a strong reduction in recycling and degradation. We therefore speculate that the Rab4 protein performs an important role in the normal functioning of the early sorting endosome, possibly controlling the formation of membrane buds destined for transport to both recycling and degradative acceptor compartments. The isolation of Rab4 interacting proteins [32,42–45] and the development of in vitro assays to study Rab4 function will facilitate future studies for the elucidation of the molecular mechanism of action of this GTPase.

Acknowledgements: This project was supported, in part, by Grants from the European Community (No. ERBCHRXCT940592 to M.W.M. and No. ERBFMRXCT960020 to M.W.M. and C.B.) and from the Italian Consiglio Nazionale per le Ricerche (Progetto Finalizzato Biotecnologie to C.B.). The authors wish to thank Gerd Sutter for gift of the MVA T7 vaccinia virus and Harald Stenmark for the gift of the anti-EEA1 antibody. We thank Bruno Goud and Marino Zerial for encouragement and stimulating discussions over the years. We also are very grateful to John P. Fraher, Bereniece Rea, Peter Dockery, Anatomy Department, UCC for use of the confocal microscope, technical assistance in confocal imaging and useful discussions.

References

[1] Mukherjee, S., Ghosh, R.N. and Maxfield, F.R. (1997) Physiol. Rev. 77, 759–803.
[2] Trowbridge, I.S., Collawn, J.F. and Hopkins, C.R. (1993) Annu. Rev. Cell Biol. 9, 129–161.
[3] Gruenberg, J. and Maxfield, F.R. (1995) Curr. Opin. Cell Biol. 7, 552–563.
[4] Mellman, I. (1996) Annu. Rev. Cell Dev. Biol. 12, 575–625.
[5] Ghosh, R.N. and Maxfield, F.R. (1995) J. Cell Biol. 128, 549–561.
[6] Hopkins, C.R., Gibson, A., Shipman, M., Strickland, D.K. and Trowbridge, I.S. (1994) J. Cell Biol. 125, 1265–1274.
[7] Yamashiro, D.J., Tycko, B., Fluss, S.R. and Maxfield, F.R. (1984) Cell 37, 789–800.
[8] Rothman, J.E. (1994) Nature 372, 55–63.
[9] Rothman, J.E. and Warren, G. (1994) Curr. Biol. 4, 220–233.
[10] Olkkonen, V.M. and Stenmark, H. (1997) Int. Rev. Cytol. 176, 1–85.
[11] Pfeffer, S.R. (1999) Nat. Cell Biol. 1, 17–22.
[12] Martinez, O. and Goud, B. (1998) Biochim. Biophys. Acta 1404, 101–112.
[13] Novick, P. and Zerial, M. (1997) Curr. Opin. Cell Biol. 9, 496–504.
[14] Goud, B. and McCaffrey, M. (1991) Curr. Opin. Cell Biol. 3, 626–633.
[15] Valencia, A., Chardin, P., Wittinghofer, A. and Sander, C. (1991) Biochemistry 30, 4637–4648.
[16] van der Sluijs, P., Hull, M., Zahraoui, A., Tavitian, A., Goud, B. and Mellman, I. (1991) Proc. Natl. Acad. Sci. USA 88, 6313–6317.

[17] van der Sluijs, P., Hull, M., Webster, P., Male, P., Goud, B. and Mellman, I. (1992) Cell 70, 729–740.
[18] Gorvel, J.P., Chavrier, P., Zerial, M. and Gruenberg, J. (1991) Cell 64, 915–925.
[19] Bucci, C., Parton, R.G., Mather, I.H., Stunnenberg, H., Simons, K., Hoflack, B. and Zerial, M. (1992) Cell 70, 715–728.
[20] Stenmark, H., Parton, R.G., Steele-Mortimer, O., Lutcke, A., Gruenberg, J. and Zerial, M. (1994) EMBO J. 13, 1287–1296.
[21] McLauchlan, H., Newell, J., Morrice, N., Osborne, A., West, M. and Smythe, E. (1998) Curr. Biol. 8, 34–45.
[22] Ullrich, O., Reinsch, S., Urbe, S., Zerial, M. and Parton, R.G. (1996) J. Cell Biol. 135, 913–924.
[23] Wilcke, M., Johannes, L., Galli, T., Mayau, V., Goud, B. and Salamero, J. (2000) J. Cell Biol. 151, 1207–1220.
[24] Chavrier, P., Parton, R.G., Hauri, H.P., Simons, K. and Zerial, M. (1990) Cell 62, 317–329.
[25] Lombardi, D., Soldati, T., Riederer, M.A., Goda, Y., Zerial, M. and Pfeffer, S.R. (1993) EMBO J. 12, 677–682.
[26] Meresse, S., Gorvel, J.P. and Chavrier, P. (1995) J. Cell Sci. 108, 3349–3358.
[27] Feng, Y., Press, B. and Wandinger-Ness, A. (1995) J. Cell Biol. 131, 1435–1452.
[28] Vitelli, R., Santillo, M., Lattero, D., Chiariello, M., Bifulco, M., Bruni, C.B. and Bucci, C. (1997) J. Biol. Chem. 272, 4391–4397.
[29] Bucci, C., Thomsen, P., Nicoziani, P., McCarthy, J. and van Deurs, B. (2000) Mol. Biol. Cell 11, 467–480.
[30] Daro, E., van der Sluijs, P., Galli, T. and Mellman, I. (1996) Proc. Natl. Acad. Sci. USA 93, 9559–9564.
[31] Bottger, G., Nagelkerken, B. and van der Sluijs, P. (1996) J. Biol. Chem. 271, 29191–29197.
[32] Vitale, G., Rybin, V., Christoforidis, S., Thornqvist, P., McCaffrey, M., Stenmark, H. and Zerial, M. (1998) EMBO J. 17, 1941–1951.
[33] Touchot, N., Chardin, P. and Tavitian, A. (1987) Proc. Natl. Acad. Sci. USA 84, 8210–8214.
[34] Sutter, G., Ohlmann, M. and Erfle, V. (1995) FEBS Lett. 371, 9–12.
[35] Bucci, C., Lutcke, A., Steele-Mortimer, O., Olkkonen, V.M., Dupree, P., Chiarello, M., Bruni, C.B., Simons, K. and Zerial, M. (1995) FEBS Lett. 366, 65–71.
[36] Papini, E., Satin, B., Bucci, C., de Bernard, M., Telford, J.L., Manetti, R., Rappuoli, R., Zerial, M. and Montecucco, C. (1997) EMBO J. 16, 15–24.
[37] Bradford, M.M. (1976) Anal. Biochem. 72, 248–254.
[38] Mu, F.T., Callaghan, J.M., Steele-Mortimer, O., Stenmark, H., Parton, R.G., Campbell, P.L., McCluskey, J., Yeo, J.P., Tock, E.P. and Toh, B.H. (1995) J. Biol. Chem. 270, 13503–13511.
[39] Trischler, M., Stoorvogel, W. and Ullrich, O. (1999) J. Cell Sci. 112, 4773–4783.
[40] Sonnichsen, B., De Renzis, S., Nielsen, E., Rietdorf, J. and Zerial, M. (2000) J. Cell Biol. 149, 901–914.
[41] Chavrier, P., van der Sluijs, P., Mishal, Z., Nagelkerken, B. and Gorvel, J.P. (1997) Cytometry 29, 41–49.
[42] Nagelkerken, B., Van Anken, E., Van Raak, M., Gerez, L., Mohrmann, K., Van Uden, N., Holthuizen, J., Pelkmans, L. and Van Der Sluijs, P. (2000) Biochem. J. 346, 593–601.
[43] Li, L., Omata, W., Kojima, I. and Shibata, H. (2000) J. Biol. Chem. 3, 3.
[44] Cormont, M., Mari, M., Galmiche, A., Hofman, P. and Le Marchand-Brustel, Y. (2001) Proc. Natl. Acad. Sci. USA 98, 1637–1642.
[45] Bielli, A., Thörnqvist, P.O., Hendrick, A.G., Finn, R., Fitzgerald, K. and McCaffrey, M.W. (2001) Biochem. Biophys. Res. Commun., in press.